# Interpretation of Coastal HF Radar–Derived Surface Currents with High-Resolution Drifter Data

CARTER OHLMANN,*,+ PETER WHITE,* LIBE WASHBURN,# ERIC TERRILL,+ BRIAN EMERY,# AND MARK OTERO+

* *Institute for Computational Earth System Science, University of California, Santa Barbara, Santa Barbara, California*
+ *Scripps Institution of Oceanography, La Jolla, California*
# *Marine Science Institute, University of California, Santa Barbara, Santa Barbara, California*

(Manuscript received 2 March 2006, in final form 12 June 2006)

ABSTRACT

Dense arrays of surface drifters are used to quantify the flow field on time and space scales over which high-frequency (HF) radar observations are measured. Up to 13 drifters were repetitively deployed off the Santa Barbara and San Diego coasts on 7 days during 18 months. Each day a regularly spaced grid overlaid on a 1-km$^2$ (San Diego) or 4-km$^2$ (Santa Barbara) square, located where HF radar radial data are nearly orthogonal, was seeded with drifters. As drifters moved from the square, they were retrieved and replaced to maintain a spatially uniform distribution of observations within the sampling area during the day. This sampling scheme resulted in up to 56 velocity observations distributed over the time (1 h) and space (1 and 4 km$^2$) scales implicit in typical surface current maps from HF radar. Root-mean-square (RMS) differences between HF radar radial velocities obtained using measured antenna patterns, and average drifter velocities, are mostly 3–5 cm s$^{-1}$. Smaller RMS differences compared with past validation studies that employ current meters are due to drifter resolution of subgrid-scale velocity variance included in time and space average HF radar fields. Roughly 5 cm s$^{-1}$ can be attributed to sampling on disparate time and space scales. Despite generally good agreement, differences can change dramatically with time. In one instance, the difference increases from near zero to more than 20 cm s$^{-1}$ within 2 h. The RMS difference and bias (mean absolute difference) for that day exceed 7 and 12 cm s$^{-1}$, respectively.

## 1. Introduction

Remote sensing of near-surface currents with high-frequency (HF) radar was demonstrated more than 30 yr ago by Stewart and Joy (1974). The measurement is based on the fact that electromagnetic radiation in the 3- to 30-MHz range scatters strongly (Bragg scattering) from ocean surface gravity waves. The returned energy spectrum thus indicates movement of ocean surface gravity waves with a wavelength of half the radar-transmitted wavelength in directions either toward or away from the HF radar site (radial directions). Subtraction of the theoretical phase velocity of the ocean waves gives radial current velocities (hereafter referred to as radials). Multiple radars are typically deployed so radials have enough angular separation to resolve both the north–south and east–west velocity components (hereafter referred to as totals).

Two HF radar technologies are commonly used for oceanographic research. Beam-forming radars electronically point linear arrays of receive antennas to determine bearing over the sea surface. Examples include the Ocean Surface Current Radar (OSCR; Hammond et al. 1987) and the Wellen radar (WERA; Gurgel et al. 1999). Direction-finding radars rely on directional properties of antenna elements to determine bearing. The most commonly employed direction-finding radar, and the one from which radar data presented here come, is the Seasonde, which uses two directional antennas and a monopole antenna (Barrick and Lipa 1997).

Spatial coverage of HF radar measurements varies according to transmit frequency. For the ~25- and ~12-MHz systems reported on here, maximum ranges are ~42 and ~83 km, respectively. Environmental conditions such as the occurrence of radio interference and

*Corresponding author address:* Dr. Carter Ohlmann, Institute for Computational Earth System Science, University of California, Santa Barbara, Santa Barbara, CA 93106.
E-mail: carter@icess.ucsb.edu

DOI: 10.1175/JTECH1998.1

(occasionally) a lack of Bragg scattering ocean waves also affect range. The water depth over which the HF radar measurement integrates depends on wavelength of the Bragg scattering gravity waves, and is 0.5–1.0 m for the radars used here. Radials are obtained from cross-spectra computed between voltage time series from the elements of the receive antenna as described by Barrick and Lipa (1997) based on the MUSIC algorithm of Schmidt (1986). Estimating cross-spectra from signal voltage time series between antennas requires time averaging, typically ranging from several minutes to about an hour, depending on radar operating parameters. More detailed descriptions of HF radar technology are given in Barrick et al. (1974), Stewart and Joy (1974), Barrick et al. (1977), Frisch and Weber (1980), and Shay et al. (1995). Typically, HF radar current measurements are given as hourly averages interpolated onto 1- to 2-km square grids.

A number of calibration and validation studies have examined the ability of HF radars to measure surface currents. Initially, HF radar physics were validated through comparisons with surface velocities from drifting buoys (hereafter drifters). Stewart and Joy (1974) compared velocities from the tracks of six drifters (drogued at 1- and 4-m depth) with HF radar–derived currents, and found agreement to "a few centimeters per second" after accounting for Doppler resolution errors of at least a few centimeters per second. The HF radar comparisons with drifter and cork float velocities performed by Barrick et al. (1977) showed a root-mean-square (RMS) difference of 27 cm $s^{-1}$. Although these studies used data from multiple drifters, comparisons were with drifter velocities calculated for a single change in position of a single drifter, and not with time and space averages determined from the set of drifter tracks.

Moored current meter and profiler data have also been used for validation. Differences between HF radar– and current meter–derived velocities near 10–15 cm $s^{-1}$ have been reported by Holbrook and Frisch (1981), Janopaul et al. (1982), and Schott et al. (1986). More recently, Chapman et al. (1997) used shipborne current meter data to suggest the upper bound of HF radar accuracy is 7–8 cm $s^{-1}$. Paduan and Rosenfeld (1996) used both ADCP and drifter data to show that RMS differences with HF radar data are 10 to more than 20 cm $s^{-1}$. The most recent comparisons between HF radar velocities and point measurements show RMS differences between 7 and 19 cm $s^{-1}$ (Kohut and Glenn 2003; Emery et al. 2004; Kaplan et al. 2005; Paduan et al. 2007).

Differences between surface current velocities from HF radar and other platforms are expected for a number of reasons (e.g., Barrick et al. 1977; Graber et al. 1997). First, measurements from HF radar, drifters, and current meters are all inexact. The frequency resolution of computed radar cross-spectra, which depends on FFT length, limits radial velocity resolution to ~5 and 2.5 cm $s^{-1}$ for 12- and 25-MHz systems, respectively. Drifters can slip at ~1 to 2 cm $s^{-1}$ from the ocean water they follow (Ohlmann et al. 2005). Second, vertical scales of measurement differ. The HF radar gives vertically integrated values from the surface, drifters give integrated values over their drag elements, and current meters give values for specific depths or depth bins. Third, horizontal scales of measurement differ. Typically, HF radars average over extensive horizontal areas (up to several $km^2$), while other platforms give point measurements or limited spatial measurements following motion. Fourth, measurements are not necessarily coincident in time. Finally, Stokes drift may not be reconciled consistently among platforms.

Past HF radar validation studies have not used observations to address how differing horizontal scales of measurement manifest themselves in comparisons. In this study, HF radar–derived velocities (radials and totals) are compared with velocity estimates from large numbers of simultaneous drifter observations. Drifter averages are obtained within an area observed by HF radar, thus allowing comparison of velocity estimates on similar time and space scales. The primary goal of this study is to quantify the effects of spatial averaging, over various scales, on measurement differences between HF radar and drifter velocities. A secondary goal is to demonstrate the sort of subgrid-scale motions that are averaged in HF radar velocity products. The paper is organized as follows. The HF radar and drifter data used in the study are presented in section 2. Drifter velocities are compared with HF radar radials and totals in section 3. The comparisons are discussed, and conclusions are stated in section 4.

## 2. Observations and methods

### *a. Santa Barbara Channel HF radar data*

The HF radar data in the Santa Barbara Channel have been collected with up to five SeaSondes (manufactured by CODAR Ocean Sensors, Ltd., Los Altos, California) from 1997 to the present. A detailed description of the Santa Barbara Channel HF radar data is given by Emery et al. (2004). Data used in this study come from SeaSondes located at Coal Oil Point (COP) and Refugio State Beach (RFG), which transmit at 13.49 and 12.20 MHz, respectively, and receive backscatter signals from ocean surface waves with Bragg

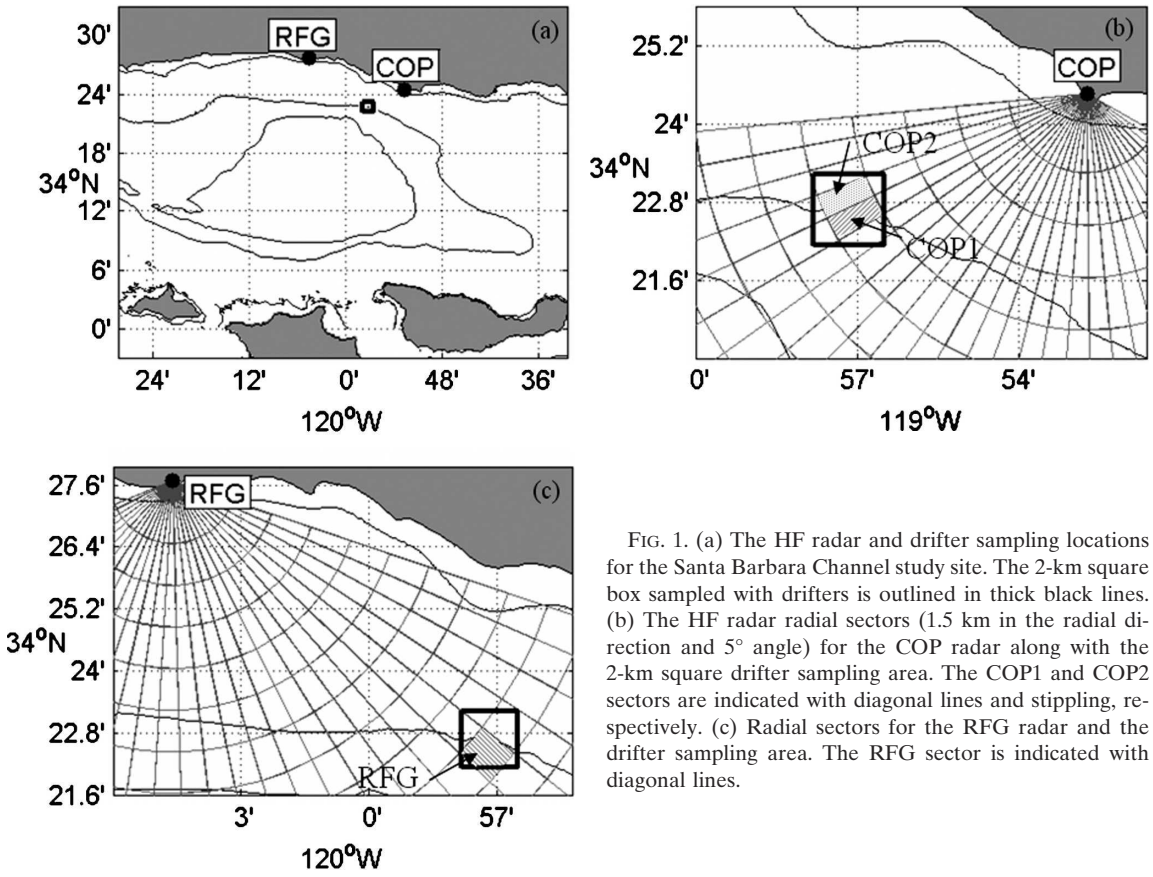


FIG. 1. (a) The HF radar and drifter sampling locations for the Santa Barbara Channel study site. The 2-km square box sampled with drifters is outlined in thick black lines. (b) The HF radar radial sectors (1.5 km in the radial direction and 5° angle) for the COP radar along with the 2-km square drifter sampling area. The COP1 and COP2 sectors are indicated with diagonal lines and stippling, respectively. (c) Radial sectors for the RFG radar and the drifter sampling area. The RFG sector is indicated with diagonal lines.

wavelengths ($\lambda$) of 11.1 and 12.3 m (Fig. 1). At these transmit frequencies, measured velocities are depth integrated over the top ~1 m of the ocean ($\lambda/4\pi$; Stewart and Joy 1974).

The radar coverage area is divided into concentric sectors that are 1.5 km in range by 5° in bearing, corresponding to radar resolution (Fig. 1). Sector areas increase linearly from ~0.3 to 10.8 km$^2$ as radial range increases from 1.5 (sectors nearest the radars) to 85 km (typical outer edge of the coverage area). Currents in the radial direction are computed for each sector every 10 min from the cross-spectra recorded at each SeaSonde using measured antenna patterns. The 10-min radial data are then time averaged to give hourly radials. The Santa Barbara radials used in this analysis come from sectors that are 7.5 and 15 km from the COP and RFG radars, and have areas of ~1.0 and 2.0 km$^2$, respectively (Fig. 1).

Totals giving hourly averages of both north and east velocity components on a 2-km square grid are computed from all radial data within 3 km of each grid point. This is done using the least squares method of Gurgel (1994). To reduce errors from geometric dilution of precision (GDOP; e.g., Graber et al. 1997), totals are only computed when the angle between available radial data is within the range of 60°–120°.

### *b. San Diego HF radar data*

The HF radar data off the San Diego coast have been collected with up to four SeaSondes from September 2002 to the present. Data for this study come from SeaSondes located on South Coronado Island (CI), Point Loma (PL), and at Boarder Park in Imperial Beach (BP; Fig. 2). The three units operate at 24.80, 25.27, and 25.60 MHz, respectively, roughly twice the frequency of the Santa Barbara Channel radars. Backscattered signals are received from ocean waves with wavelengths between 5.85 and 6.04 m and the depth of integration is ~0.5 m. The Bragg scattering wavelengths and integration depths are nearly half those in Santa Barbara owing to the higher radio frequencies. Radials in San Diego are also recorded every 10 min for sectors that are 1.5 km in range by 5° in bearing using measured antenna patterns (Fig. 2). Hourly radials are computed from the 10-min data. San Diego radials analyzed here are from sectors that are roughly 14.7, 13.2,

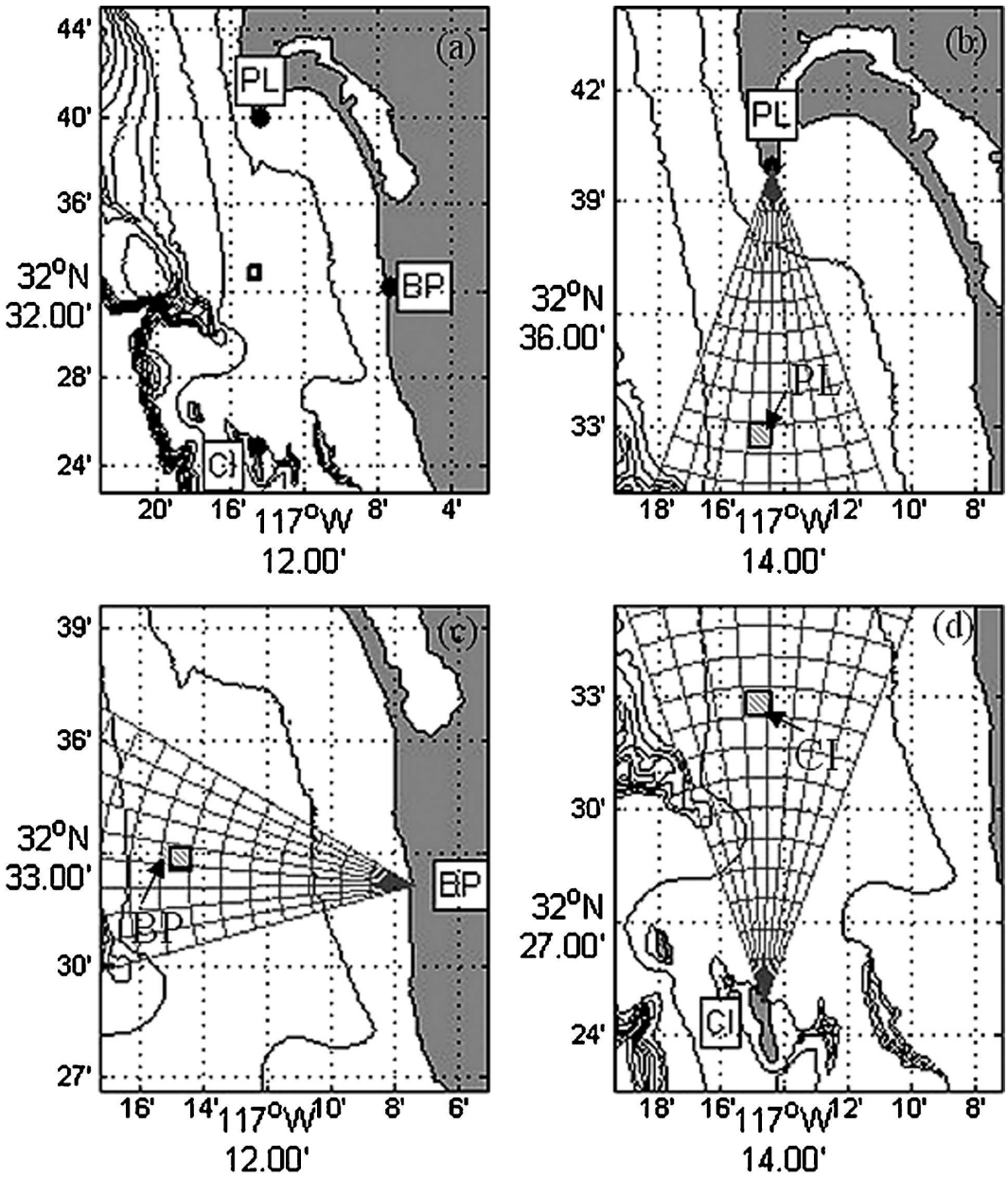


FIG. 2. As in Fig. 1, but for the San Diego study site. The box sampled with drifters is 1 km square. Radial data are from sectors filled with diagonal lines and labeled (b) PL, (c) BP, and (d) CI.

and 11.6 km from the CI, PL, and BP radars, and have areas of ~1.9, 1.7, and 1.5 km$^2$, respectively.

Hourly totals in San Diego are computed identically to the Santa Barbara totals, but on a 1-km square grid, using radials within 1.5 km of each grid point. The San Diego SeaSondes were operated in a higher-resolution mode, allowing currents to be computed on a higher-resolution grid compared with Santa Barbara. Analyses that follow are on a variety of spatial scales corresponding to the highest resolution HF radar data available.

### *c. Drifter data*

Drifter data used in this study are collected with global positioning system (GPS) located, reusable, cellular instruments developed for high-resolution nearshore use (Ohlmann et al. 2005). The drifters (manufactured by Pacific Gyre Corporation, Oceanside, California) are comprised of a corner-radar-reflector–type drogue attached to a surface float that houses the electronics. The drogue is roughly 85 cm in diameter, and is

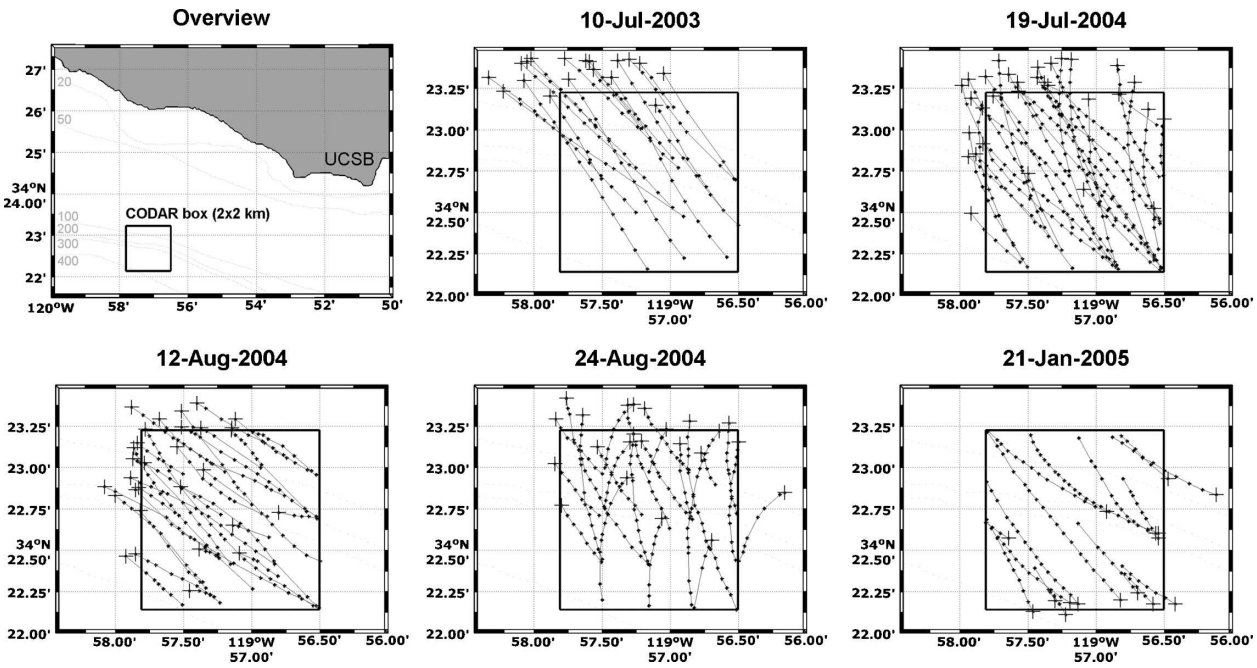


FIG. 3. Drifter data collected in the Santa Barbara HF radar domain. Dots comprising each drifter track show position sampled with GPS every 10 min (nominally). Plus signs indicate final positions. (a) Sampling location relative to the coast (see also Fig. 1). Data were collected on (b) 10 Jul 2003, (c) 19 Jul 2004, (d) 12 Aug 2004, (e) 24 Aug 2004, and (f) 21 Jan 2005.

centered at a depth near 1 m. The surface float is ~20 cm in diameter giving a drag-area ratio greater than 41 (Niiler et al. 1995). The drifters determine their position, accurate to within a few meters, every 10 min with GPS. Position data are transmitted in near real-time using the Mobitex terrestrial cellular communications system, a text messaging–type network. Accurate near–real time positions allow recovery and redeployment of the drifters. The drifters follow the water to within ~1 to 2 cm $s^{-1}$ and experience vertical shears of 1 to 2 cm $s^{-1}$ from the top to bottom of the drogue (Ohlmann et al. 2005). Observed error (standard deviation) in drifter position is responsible for a corresponding error in velocity less than 1 cm $s^{-1}$ for the 10-min sampling interval (Ohlmann et al. 2005).

### 1) SANTA BARBARA DRIFTER DATA

Drifter experiments were designed to obtain average current velocities from as many drifter observations as possible on the time (1 h) and space (1–4 $km^2$) scales resolved by the HF radars. In the Santa Barbara Channel a set of up to 13 drifters was repetitively deployed at regularly spaced 0.5-km grid points within a 2 km × 2 km box (hereafter total box) located where radials from the COP and RFG radars are most orthogonal (Fig. 1). The deployment location was chosen to minimize GDOP errors. The grid spacing was selected to position drifters uniformly within the box and allow for multiple position records prior to exit. Maintaining 13 drifters in the total box proved to be on the upper edge of what can be managed by a single skiff for current speeds near 30 cm $s^{-1}$ in the prevailing wind and wave conditions of the Santa Barbara Channel.

Grid points initially selected for deployments (out of a possible 25) within the total box were those located farthest upcurrent as determined from recent HF radar observations. As the drifters moved downcurrent and out of the total box, they were recovered and redeployed at grid points farthest from drifters already in the box, and sufficiently far upcurrent to ensure multiple subsequent position records within the box. Drifters were repetitively redeployed for 5 to 8 h, depending on wind and sea conditions. Velocities were computed from 10 min (nominally) drifter positions as first differences and decomposed into radial and total components.

Santa Barbara Channel drifter deployments occurred on 5 days between 10 July 2003 and 21 January 2005 (Fig. 3; Table 1). The 10 July 2003 deployment was one of the first uses of the drifters and occurred during the manufacturer's instrument evaluation period. Only seven drifters were deployed to ensure fleet management while working out retrieval and redeployment logistics. A total of 124 velocity observations were col-

TABLE 1. Drifter sampling statistics summary. Sampling date (column 1). Total number of drifters utilized (column 2). Total number of drifter tracks collected considering drifter retrieval and redeployment (column 3). Total number of velocity observations computed from first differences in the 10 min position data in the total box seeded (column 4). Time (min) between deployment of the first drifter to retrieval of the final drifter (column 5). The first five rows correspond to deployments in Santa Barbara; the last two correspond to deployments in San Diego.

| Date | No. drifters deployed | No. drifter tracks | No. velocity observations | Sampling time (min) |
|---|---|---|---|---|
| 7 Oct 2003 | 7 | 18 | 124 | 310 |
| 19 Oct 2004 | 13 | 31 | 314 | 440 |
| 12 Aug 2005 | 12 | 30 | 208 | 351 |
| 24 Aug 2004 | 10 | 23 | 211 | 327 |
| 21 Jan 2005 | 6 | 16 | 137 | 320 |
| 13 Apr 2005 | 8 | 16 | 109 | 202 |
| 14 Apr 2005 | 7 | 17 | 131 | 258 |

lected showing northwest (upcoast) movement near 40 cm $s^{-1}$ (Fig. 3b). The second deployment occurred more than a year later (19 July 2004) after redesigning some of the drifter electronics and firmware. A total of 314 velocity observations collected with 13 drifters show mean upcoast currents with velocity near 23 cm $s^{-1}$ (Fig. 3c). The third and fourth deployments on 12 and 24 August 2004 each yielded just over 200 velocity observations with mean upcoast currents near 24 (Fig. 3d) and 17 cm $s^{-1}$ (Fig. 3e), respectively. The fifth and final deployment on 21 January 2005 was carried out with only six drifters as part of the fleet had been moved to San Diego. The 137 velocity observations show a mean downcoast current near 19 cm $s^{-1}$ (Fig. 3f). Currents observed with drifters are consistent with the large-scale Santa Barbara Channel circulation modes given by Winant et al. (2003).

#### 2) SAN DIEGO DRIFTER DATA

The San Diego drifter deployment scheme is based on the same idea of keeping an HF radar grid box populated with drifters as best as possible during the course of a day, but the total box is 1-km square and drifters were deployed on a 0.2-km square grid within the box. Drifter sampling is denser than at Santa Barbara corresponding to the higher spatial resolution of the San Diego radars. The drifter deployment location was chosen as the midpoint of the baseline between the PL and CI SeaSondes so between-radar assessments could be made along with drifter validation efforts at the radial level. Radials from the BP SeaSonde are nearly orthogonal at the selected location (Fig. 2).

Drifter sampling in San Diego occurred on two consecutive days. A total of eight drifters were used to collect 109 velocity observations over 3.3 h on 13 April 2005 (Table 1). The drifters generally move to the southwest with a velocity near 10 cm $s^{-1}$, but change direction toward the northwest at the very end of the sampling period (Fig. 4b). On 14 April 2005 a total of seven drifters yielded 131 velocity observations showing southerly flow with a mean speed near 16 cm $s^{-1}$ (Table 1; Fig. 4c). The southerly motion is consistent with wind forcing in the region discussed by Roughan et al. (2005).

Keeping drifters within the smaller 1-km grid box during San Diego deployments was more difficult than managing drifters in Santa Barbara, despite weaker currents and generally calmer conditions. This was due to the San Diego grid comprising one-quarter of the area of the Santa Barbara grid. A smaller drifter fleet (eight units) was thus utilized.

## 3. Drifter and HF radar–derived velocity comparisons

### *a. Comparison with radials—Santa Barbara*

Hourly average radial velocities recorded in two sectors with the COP radar (Fig. 1b) and in one sector with the RFG radar (Fig. 1c) are compared with hourly average radial velocity components computed from coincidently sampled drifter observations during 33 h distributed over 5 days (Fig. 5). Hourly averaged HF radar data are by far the most commonly used and thus the most important to interpret. Comparisons are quantified as both a bias

$$\text{bias} = \langle (u_{\text{radial}} - \langle u_{\text{drifter}} \rangle) \rangle \tag{1}$$

and RMS difference

$$\text{RMS} = \sqrt{\langle (u_{\text{radial}} - \langle u_{\text{drifter}} \rangle)^2 \rangle}, \tag{2}$$

where and $u_{\text{drifter}}$ represent velocities in the radial direction obtained from radar and drifter data, respectively, and the angle brackets $\langle \cdot \rangle$ indicate an average quantity in both time and space. The three sectors considered lie almost entirely within the 2-km total grid box. The short range from the COP radar results in two sectors being contained in the total box, referred to as COP1 and COP2 (Fig. 1b). Drifter data within a sector are sometimes limited. Considering drifter data collected outside but near each sector gives greater opportunity for comparison, but with reduced spatial correspondence. Nearby data are included in the descriptive comparison (Fig. 5), but not in comparison statistics.

On 10 July 2003, the COP radar gives radial velocities near $-10$ cm $s^{-1}$ at 1700 UTC for both radial cells con-

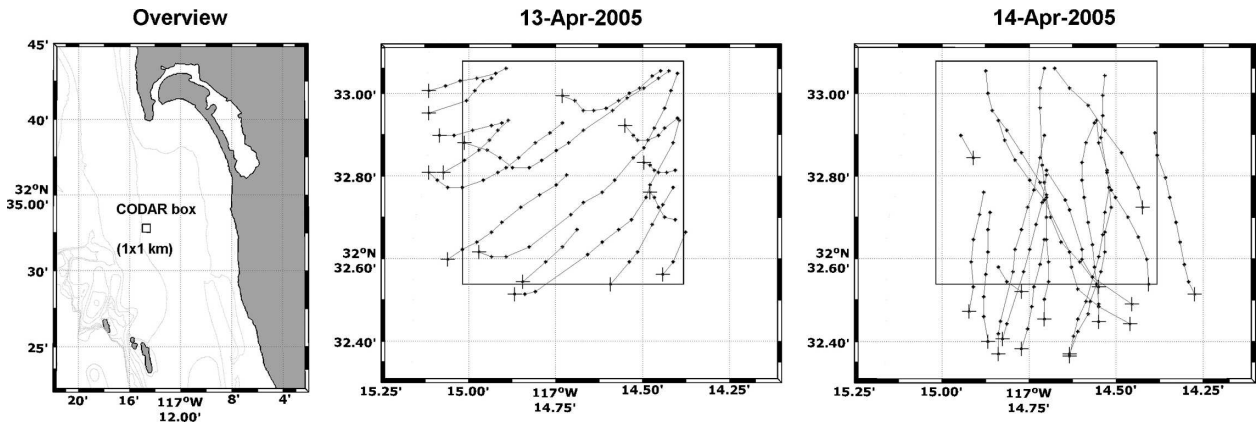


FIG. 4. As in Fig. 3, but for the San Diego study site. (a) Sampling location (see also Fig. 2). Data were collected on (b) 13 Apr 2005 and (c) 14 Apr 2005.

sidered (Fig. 5). The velocity increases to $-20$ cm s$^{-1}$ at 1800 UTC, and then decreases to near $-5$ cm s$^{-1}$ from 1900 to 2200 UTC. The radial component of drifter velocities shows the same general pattern: an increase in magnitude from near $-10$ to $-20$ cm s$^{-1}$, followed by a decrease and leveling off near $-5$ cm s$^{-1}$. In all hourly bins where at least four drifter velocity observations exist, the HF radar velocity lies within the spread of drifter data. The average drifter spread, computed as the mean hourly standard deviation in the radial component of drifter velocities within the COP radial sectors are 1.9 and 3.2 cm s$^{-1}$ for COP1 and COP2, respectively (Table 2a). The average differences between the most extreme hourly values are 4.6 and 9.0 cm s$^{-1}$ (Table 2b). The average hourly RMS differences between drifter and HF radar radials are 1.4 and 3.6 cm s$^{-1}$ for the two sectors (Table 3a). The average biases, computed as a mean of differences between the mean of drifter values for an hour and the corresponding HF radar value [Eq. (1)], are 1.4 and 3.5 cm s$^{-1}$ for the COP radials on 10 July 2003 (Table 3b).

The HF radar radial velocities from both COP radial sectors are also in good agreement with drifter data on 19 July, 12 August, and 24 August 2004 (Fig. 5). On 19 July, velocities increase from near $-5$ to $-10$ cm s$^{-1}$, and then change direction to 10 cm s$^{-1}$. On 12 August, velocities are more constant staying mostly between $-5$ and $-15$ cm s$^{-1}$. On 24 August, velocities change nearly 30 cm s$^{-1}$, from more than $-10$ to nearly 20 cm s$^{-1}$ during the 6-h sampling period. Both HF radar and drifter data capture the hourly velocity evolution during these times. The average standard deviation for hourly averages in drifter velocities ranges from 1.7 to 3.0 cm s$^{-1}$ (Table 2a). The average hourly maximum spread is between 4.8 and 9.6 cm s$^{-1}$ (Table 2b). RMS differences between HF radar and drifter velocities extend from 2.4 to 7.8 cm s$^{-1}$, and associated biases are between 0.1 and 7.4 cm s$^{-1}$ (Table 3). Differences between HF radar and drifter values are, on average, smaller than reported in past validation studies, which failed to account for spatial variation in velocities.

The HF radar velocities almost always lie within the spread of 10-min drifter observations in comparisons for the COP1 sector on 19 July and 12 August, but rarely lie within the drifter spread for COP2 (Fig. 5). The drifter data show similar flow statistics for the two radial cells in any given hour (Table 2; means within 2–3 cm s$^{-1}$). However, the HF radar values can differ dramatically between adjacent sectors (more than 12 cm s$^{-1}$ during hour 1900 on 12 August; Fig. 5).

The COP radial velocities are in poor agreement with drifter observations on 21 January (Fig. 5). The average standard deviation and spread computed from drifter data for the day are 1.9 and 4.8 cm s$^{-1}$, respectively, typical of the flow characteristics observed in the region (Table 2). However, HF radar velocities consistently lie well outside the range of drifter scatter and are consistently larger than mean hourly drifter observations by $\sim$9 cm s$^{-1}$ (Table 3a). These large differences may result from antenna pattern distortions, which can produce angular biases in observations (Kohut and Glenn 2003; Emery et al. 2004). Antenna patterns measured at COP changed between 7 May 2004 and 18 August 2005; however, raw data are unavailable for reprocessing. Comparisons between drifter velocities and HF radar radials from adjacent sectors do not show a significant improvement in correlation for any of the sampling days.

Data collected in a single sector with the RFG radar and the corresponding radial component from drifter data generally show larger velocities than for the COP radials. The RFG radar location relative to the sector

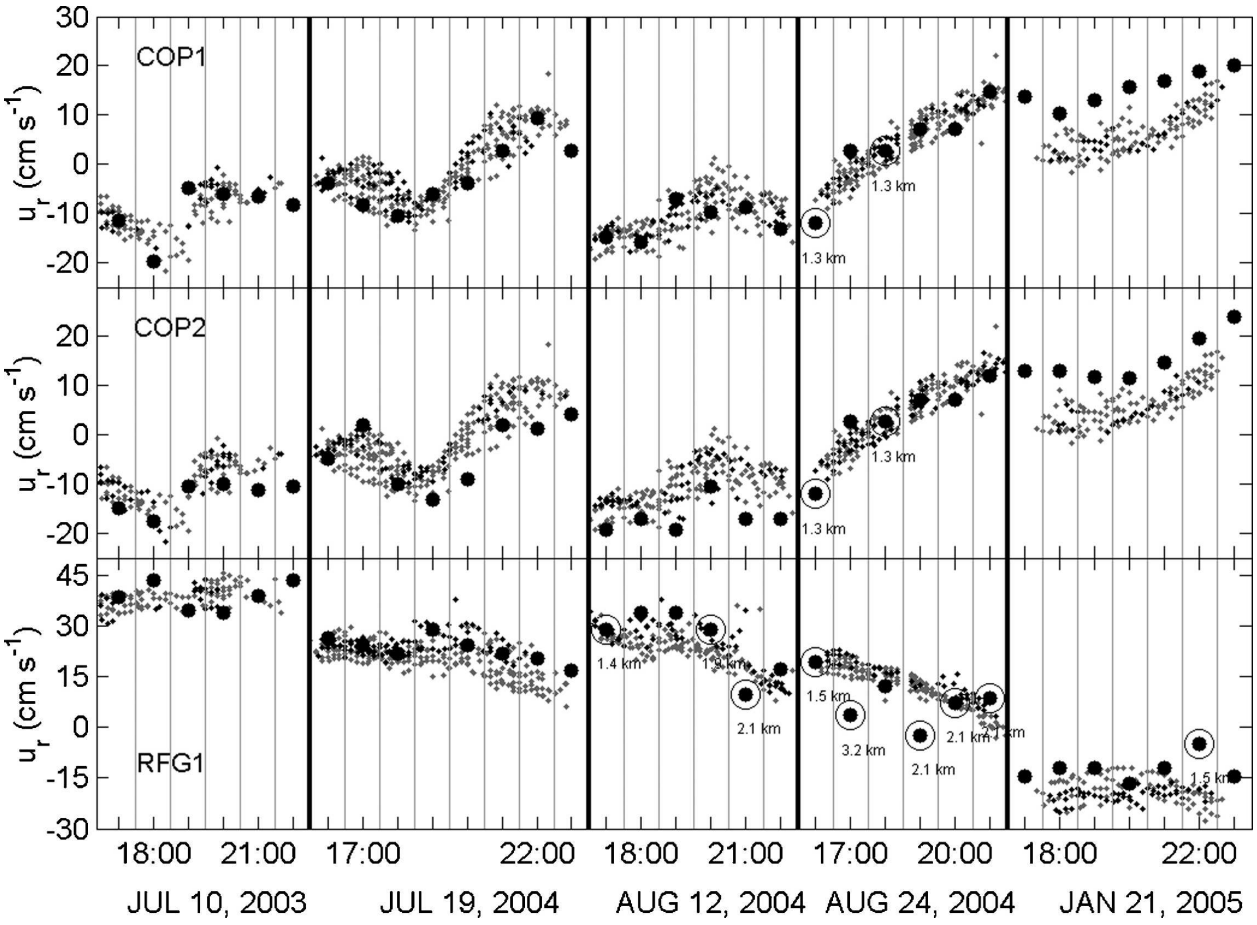


FIG. 5. Time series of HF radar radials and corresponding drifter velocities collected in Santa Barbara. The HF radar values (large black dots) are hourly average radials for the (top) COP1, (middle) COP2, and (bottom) RFG sectors (see Fig. 1). Drifter values are the radial component of velocities collected within each sector (small black dots), and outside the sector but within the 2-km square total box seeded (small gray dots). The HF radar values from distant sectors are circled and labeled with the distance away. Velocity comparisons are shown for multiple hours on five different days. Horizontal gray lines delineate hourly periods over which HF radar values are averaged. Horizontal black lines delineate days. The velocity scale changes between panels. Times are in UTC.

being considered (labeled RFG in Fig. 1) results in radial components with a larger projection in the alongshore direction, the generally dominant direction of coastal flows (Csanady 1982). On 10 July 2003 RFG radial velocities and associated drifter data show relatively constant velocities between 35 and 45 cm s$^{-1}$ (Fig. 5). The standard deviation for the radial component of drifter observations is 3.4 cm s$^{-1}$, slightly larger than values for the COP radial cells and consistent with observed high frequency variations in the alongshore velocity component (Table 2; Ohlmann et al. 2005). The RMS difference between hourly HF radar and drifter velocities is 3.3 cm s$^{-1}$, consistent with COP values, despite fewer hours where the radial sector is heavily seeded with drifters (Fig. 5). Velocity data for the RFG sector on 19 July show a slight decreasing trend throughout the day. The standard deviation in drifter data is 2.7 cm s$^{-1}$ and the hourly HF radar values lie mostly within the spread of coincident drifter observations giving an RMS difference between HF radar and drifter velocities of 2.1 cm s$^{-1}$ (Table 3a).

After 19 July, the RFG radar intermittently sampled the sector considered, producing many data gaps. For comparison with drifters during gaps, radials are taken from the nearest sector with available data. These values are circled in Fig. 5, and their distance from the center of the total box seeded with drifters is noted (1.3–3.2 km). Inclusion of the outlying radials allows a limited qualitative comparison between drifter and HF radar data that are not collocated. On 12 and 24 August, 8 of the 12 radials available from the RFG radar are from outlying sectors. Of these eight, only three clearly lie within the spread of drifter observations indicating no obvious improvement in agreement for data

TABLE 2. (a) Standard deviation (cm $s^{-1}$) of drifter velocities collected in a radial sector (columns) for a day (rows). Standard deviations are computed for each hour, and hourly values are averaged together for a day. COP is the mean for both the COP1 and COP2 sectors (Fig. 1). Velocity data used in the computation are shown in Figs. 5 and 6; (b) as in (a), but for the range of drifter velocities (max − min; cm $s^{-1}$).

| Date/station | COP1 | COP2 | COP | RFG | BP | PL | CI |
|---|---|---|---|---|---|---|---|
| (a) | | | | | | | |
| 10 Jul 2003 | 1.9 | 3.2 | 2.9 | 3.4 | — | — | — |
| 19 Jul 2004 | 3.0 | 2.1 | 2.5 | 2.7 | — | — | — |
| 12 Aug 2004 | 2.0 | 1.9 | 1.9 | 2.7 | — | — | — |
| 24 Aug 2004 | 1.7 | 1.8 | 1.8 | 0.8 | — | — | — |
| 21 Jan 2005 | 1.9 | 1.9 | 1.9 | 1.7 | — | — | — |
| 13 Apr 2005 | — | — | — | — | 2.6 | 3.3 | 3.2 |
| 14 Apr 2005 | — | — | — | — | 3.6 | 1.4 | 1.4 |
| (b) | | | | | | | |
| 10 Jul 2003 | 4.6 | 9.0 | 7.9 | 8.3 | — | — | — |
| 19 Jul 2004 | 9.6 | 6.7 | 8.0 | 8.7 | — | — | — |
| 12 Aug 2004 | 6.4 | 5.7 | 6.1 | 8.8 | — | — | — |
| 24 Aug 2004 | 4.8 | 6.7 | 6.1 | 2.2 | — | — | — |
| 21 Jan 2005 | 4.7 | 5.0 | 4.8 | 5.3 | — | — | — |
| 13 Apr 2005 | — | — | — | — | 10.8 | 12.6 | 12.2 |
| 14 Apr 2005 | — | — | — | — | 12.3 | 5.0 | 4.8 |

from offset locations. For some Santa Barbara radars, Emery et al. (2004) report higher correlations between velocities measured by current meters and HF radar for sectors distant from those containing the current meters. They speculate that antenna pointing errors in radials computed with ideal antenna patterns are the cause. Improved correlations for noncollocated data are not observed here.

### b. Comparison with radials—San Diego

Hourly radials for sectors from the BP, CI, and PL radars are compared with coincidently sampled drifter averages during 10 h over two consecutive days (Fig. 6). Distances from the radars to the total box are larger in San Diego, and the total box is smaller. Consequently, the sectors for which radials are compared are larger than the total box seeded with drifters (Fig. 2). As a result, few drifter observations lie outside the sectors used in the comparisons, but HF radar signal contributions can come from portions of the sectors not covered by the total box (i.e., without drifter sampling).

On 13 April 2005 the BP radar gives hourly radial velocities between −5 and 5 cm $s^{-1}$ reflecting weak cross-shore flow (Fig. 6). The radial component of drifter data collected every 10 min at various locations within the BP sector ranges from −2 to nearly −20 cm $s^{-1}$. The standard deviation in drifter velocities for the day, and the average range between the most extreme drifter values sampled within an hour are 2.6 and 10.8 cm $s^{-1}$, respectively (Table 2). The variance in 10-min drifter data is similar to values from the Santa Barbara Channel. Mean drifter velocities are consistently greater in the offshore direction than corresponding radar values with an RMS difference of 7.6 cm $s^{-1}$ and a mean bias of −7.2 cm $s^{-1}$ (Table 3). These are larger differences than for the Santa Barbara data, and more consistent with differences reported in previous studies (e.g., Paduan and Rosenfeld 1996; Kohut and Glenn 2003; Emery et al. 2004).

TABLE 3. (a) RMS difference (cm $s^{-1}$) between radial velocities from HF radar and drifters. The HF radar values are hourly averages by radial sector. Drifter values are means computed from all 10-min velocity observations that correspond in time and space. Daily averages are computed from hourly values. COP is the mean for both the COP1 and COP2 sectors. Only hours with more than three drifter observations distributed over at least 50% of the hour are used. For PL and CI, -I and -M indicate radar data processed with ideal and measured antenna patterns, respectively. Velocity data used in the computation are shown in Figs. 5 and 6. (b) As in (a) for the bias (cm $s^{-1}$) between HF radar and drifter derived radial velocities (radar–drifter). Positive values indicate a higher HF radar velocity in the radial direction away from the radar site.

| Date/station | COP1 | COP2 | COP | RFG | BP | PL-I | PL-M | CI-I | CI-M |
|---|---|---|---|---|---|---|---|---|---|
| (a) | | | | | | | | | |
| 10 Jul 2003 | 1.4 | 3.6 | 3.1 | 3.3 | — | — | — | — | — |
| 19 Jul 2004 | 3.8 | 5.8 | 4.9 | 2.1 | — | — | — | — | — |
| 12 Aug 2004 | 2.4 | 7.8 | 4.8 | 4.4 | — | — | — | — | — |
| 24 Aug 2004 | 4.4 | 3.1 | 3.6 | 4.4 | — | — | — | — | — |
| 21 Jan 2005 | 9.4 | 8.4 | 9.1 | 7.3 | — | — | — | — | — |
| 13 Apr 2005 | — | — | — | — | 7.6 | 13.3 | 3.2 | 9.7 | 4.6 |
| 14 Apr 2005 | — | — | — | — | 6.9 | 7.2 | 12.3 | 12.6 | 4.2 |
| (b) | | | | | | | | | |
| 10 Jul 2003 | 1.4 | 3.5 | 3.0 | −3.3 | — | — | — | — | — |
| 19 Jul 2004 | 3.7 | 4.0 | 3.8 | −0.1 | — | — | — | — | — |
| 12 Aug 2004 | 0.9 | 7.4 | 3.8 | −4.4 | — | — | — | — | — |
| 24 Aug 2004 | 0.2 | 0.1 | 0.1 | 4.4 | — | — | — | — | — |
| 21 Jan 2005 | −9.3 | −8.3 | −8.9 | −6.9 | — | — | — | — | — |
| 13 Apr 2005 | — | — | — | — | −7.2 | 10.7 | −2.7 | 9.1 | 4.0 |
| 14 Apr 2005 | — | — | — | — | −6.8 | 6.4 | 7.1 | 10.4 | 0.5 |

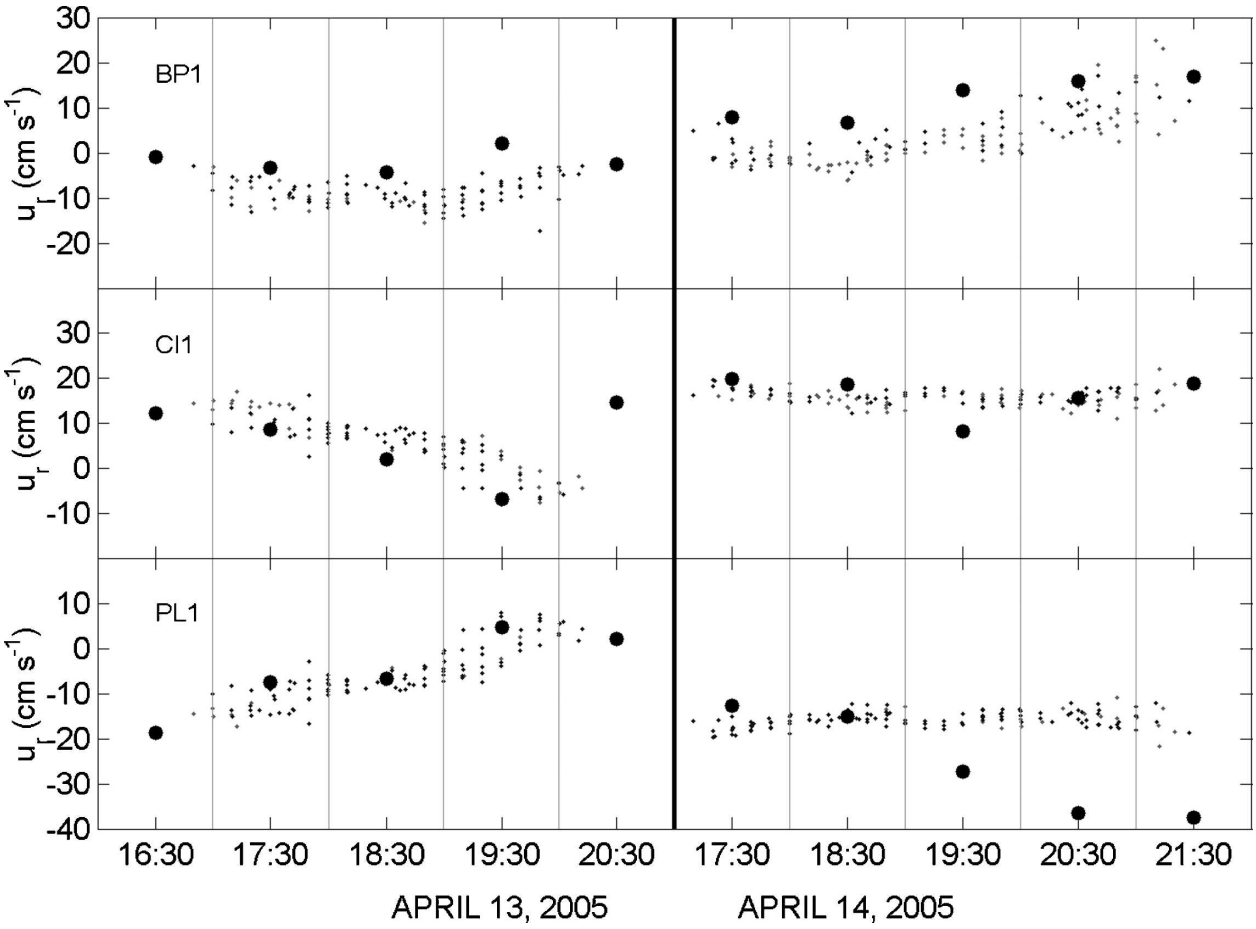


FIG. 6. As in Fig. 5, but for HF radar and drifter velocities collected in the (a) BP, (b) CI, and (c) PL sectors in San Diego (see Fig. 2).

Radial velocities from the CI and PL radars are expected to be very near equal, but of opposite sign, as their sectors nearly overlay one another along their baseline (Fig. 2). However, this is not always the case. On 13 April, the CI radar gives radials (toward the radar) that decrease from 12 to 2 cm s$^{-1}$ during the first 3 h of observations, change direction to $-7$ cm s$^{-1}$ in the fourth hour, and then reverse again and increase to near 15 cm s$^{-1}$ in the final hour (Fig. 6). Radials from the PL radar gradually change from 19 cm s$^{-1}$ (away from the radar) to 7 cm s$^{-1}$ during the first 3 h of observations. Flow direction reverses during the final 2 h and velocities are 2 to 5 cm s$^{-1}$. Radial values from the two radars are within 2 cm s$^{-1}$ at times, but differ by more than 12 cm s$^{-1}$ during the 2030 h.

Data from the radars and drifters all show the same change in currents on 13 April except for a single value from the CI radar. The CI radials give a slightly reduced southward velocity compared with the drifters and PL radials. Radials are mostly at the very edge, or just beyond, the range of drifter values (Fig. 6). The RMS difference between drifter and CI radials is 4.6 cm s$^{-1}$ and the bias is 4.0 cm s$^{-1}$ (Table 3). The PL radials are well within the spread of drifter values giving RMS difference and bias values near 3.0 cm s$^{-1}$. Variance in the radial component of the 10-min drifter velocity data is similar for both the CI and PL comparisons as expected (sectors are almost collocated) and is nearly the largest observed (standard deviation of 3.2 to 3.3 cm s$^{-1}$; Table 2).

Currents on 14 April are mostly southerly at between 15 and 20 cm s$^{-1}$ and display little finescale ($<$1 h and 1 km) variability in the alongshore direction (Fig. 4). The standard deviation for 10-min drifter observations in the direction radial to the PL and CI radars is 1.4 cm s$^{-1}$, nearly the smallest variance observed (Table 2). The standard deviation in the radial component of drifter velocity relative to the BP radar, nearly the cross-shore direction, is the largest observed in this study with a standard deviation of 3.6 cm s$^{-1}$. Drifter

velocity statistics indicate that sub–HF radar grid-scale fluctuations off the San Diego coast are not always isotropic.

Hourly radial velocities from the BP radar on 14 April generally increase throughout the day from 6 to 17 cm $s^{-1}$ (Fig. 6). These values are larger than those from drifter observations by 6.8 cm $s^{-1}$, a similar bias to that observed on the previous day (Table 3). Radial data from the CI radar lie just above the spread of drifter values during 2 h, near the center of the spread during 2 h, and below the spread during 1 h. RMS difference with mean drifter values is 4.2 cm $s^{-1}$, and the bias is less than 1 cm $s^{-1}$ (Table 3).

Perhaps the most interesting of all the comparisons are the data collected in the PL sector on 14 April. Unlike other comparisons, the HF radar and drifter data do not show similar trends throughout the day, nor is the bias constant in time (Fig. 6). Instead, the PL radial data lies outside the drifter spread during the first hour compared, showing a smaller southward velocity. Values are similar during the second hour. The PL radials then indicate a southward velocity that is more than 10 cm $s^{-1}$ greater than observed with drifters and the CI radar during the third hour, and more than 20 cm $s^{-1}$ larger during the fourth and fifth hours. The comparison gives the largest RMS difference observed between measurements (12.3 cm $s^{-1}$; Table 3). Variance in the drifter data is at a minimum for this radial component at this time (1.4 cm $s^{-1}$). The difference between aligned and nearly collocated CI and PL radials increases from ~2 cm $s^{-1}$ to more than 20 cm $s^{-1}$ over a few hours, with preferred drifter agreement for the CI data. The independent measurement provided by the drifters should allow further investigation of radar signal processing during the time of this baseline deviation.

### c. Comparison with radials—Overall

A scatterplot of all radials discussed above (large black dots in Figs. 5 and 6) and corresponding hourly mean velocities from the drifter data (hourly averages of small black dots in Figs. 5 and 6) gives an overview of measurement agreement (Fig. 7). The overall RMS difference in radial velocities is 6.5 cm $s^{-1}$. Linear least squares fits give regression lines with squared correlation coefficients ($r^2$) of 0.84 ($n = 105$).

### d. Comparison with totals—Santa Barbara

Comparison between HF radar radials and corresponding hourly average velocities from sets of coincident drifter observations allows measurement differences between instruments to be isolated. Comparison between HF radar totals and corresponding drifter velocity averages quantifies the combined influence of GDOP, spatial averaging, and measurement differences. By subsampling drifter observations used in computing average drifter velocities, the influence of disparate sampling scales in HF radar comparisons can be quantified. In addition, differences can be discussed in terms of oceanographic finescale features that are expected to be anisotropic with directionality influenced by the shoreline (Csanady 1982; Ohlmann et al. 2005).

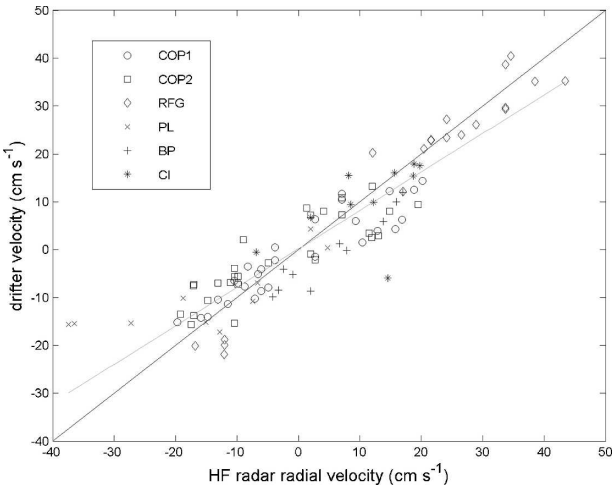


FIG. 7. Scatterplot of hourly average HF radar radials, and the corresponding (hourly and sector) average radial component of drifter velocities. Symbols correspond to the sectors from which data come (see Figs. 1 and 2). A 1–1 line is plotted in black and a best-fit linear least squares line is in gray ($r^2 = 0.84$; $n = 105$).

RMS differences in both the east–west ($u$) and north–south ($v$) velocity components between hourly average radar totals and average velocities computed from various numbers of drifter observations collected within the HF radar total box during commensurate times (hours) are calculated. Differences in Santa Barbara are computed during all hours (14 out of 33 total; $n = 14$) for which there are at least 30 drifter velocity observations in the total box. For each hour, from 1 to 30 drifter observations are randomly selected from those available and used to compute a drifter velocity average, as a function of number of drifter observations, that is compared with the radar value for that hour. Up to 56 drifter velocity observations exist within the total box during an hour. The value of 30 is selected as a trade-off between sample size and statistical reliability. A drifter velocity average from 56 observations could be computed for comparison, but this would be only for a single hour giving little statistical robustness. Statistics are then computed from the 14 difference values (hours) determined for each draw size (1 to 30).

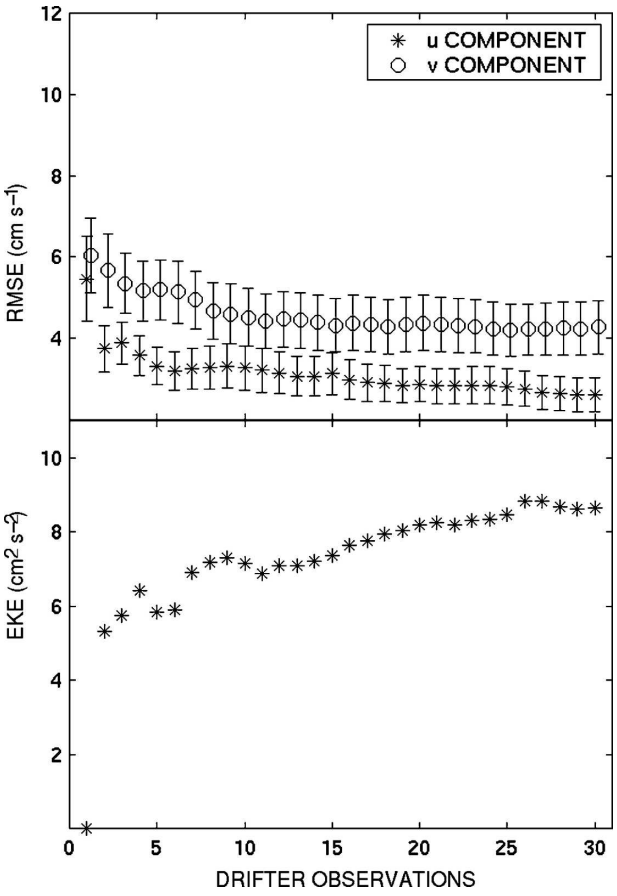


FIG. 8. RMS difference between radar and drifter total velocity components for Santa Barbara, as a function of the number of drifter observations used to compute the drifter mean (top). The HF radar totals are hourly averages within a 2-km square. Drifter velocities are corresponding time and space averages with randomly subsampled sets. The $u$ velocity component (*) is east–west and mostly alongshore in the study region. The $v$ component (o) is north–south and mostly across-shore. Error bars show standard error. The associated eddy kinetic energy (EKE) for the drifter observations used to compute drifter means in the comparisons (bottom). EKE is computed as $0.5(\langle u'u' \rangle + \langle v'v' \rangle)$, where $u'$ and $v'$ are deviations from the average u and v velocities, respectively, and the angle brackets denote mean quantities; 14 h with at least 30 drifter observations are included in the computations.

Comparison between Santa Barbara HF radar totals and hourly drifter velocities computed from 30 drifter observations within the total box gives RMS differences of 2.6 and 4.3 cm $s^{-1}$ for the $u$ (mostly alongshore in Santa Barbara) and $v$ (mostly across-shore in Santa Barbara) components, respectively (Fig. 8). As the number of drifter observations used to compute the velocity average decreases, the RMS difference between drifter and radar totals generally increases. When single drifter velocity observations are randomly selected and compared to HF radar totals for the hour, RMS difference increases to 5.5 and 6.1 cm $s^{-1}$ for the $u$ and $v$ components, respectively.

Small-scale variations in the circulation within the 4 $km^2$ total box during the course of an hour are more likely to be sampled with an increasing number of drifter observations. Therefore, average velocities incorporating a larger number of drifter observations are more likely to represent the spatial averaging of the total vector calculation for the HF radars. This accounts for the ~3.5 cm $s^{-1}$ reduction in RMS difference in velocity as the number of drifter observations increase from 1 to 30 (Fig. 8). The remaining ~3 to 4 cm $s^{-1}$ differences (i.e., RMS differences computed from 30 observations) are near those of the radial comparisons (Table 3). The asymptotic curves in Fig. 8 indicate additional drifter observations beyond ~15–20 do not reduce RMS difference as the flow field variance is sufficiently resolved in both the drifter and HF radar measurements. Discrepancies due to GDOP are expected to be small in the total box considered where radials are nearly orthogonal. Experiments with radial averaging for the formulation of totals do not lead to reduced RMS differences.

Eddy kinetic energy (EKE) computed with subsampled drifter data indicates the extent to which agreement between HF radar and average drifter velocity can be improved with additional drifter observations. EKE rises quickly to over 7 $cm^2\ s^{-2}$ with the addition of the first ~eight drifters and then asymptotes just above 8 $cm^2\ s^{-2}$ (Fig. 8). The asymptotic EKE curve indicates additional drifter observations beyond ~15–20 do not resolve additional velocity variance. The EKE curve supports the previous indication of convergence in RMS difference between platforms when the sub-HF radar grid-scale variance is resolved. More drifter observations are therefore not expected to give drifter means that improve agreement with corresponding HF radar total velocities.

### *e. Comparison with totals—San Diego*

The HF radar totals in San Diego are compared with drifter velocity averages computed over a 1-$km^2$ total box and 1 h. Average velocities are computed for hours (5) when at least 23 drifter observations are available. The smaller total box and limited deployments with fewer drifters (than for Santa Barbara) results in smaller numbers of drifters available for averaging. RMS differences between HF radar totals and average drifter velocities computed from 23 observations are 7.5 and 5.6 cm $s^{-1}$ for the $u$ (mostly across-shore in San Diego) and $v$ (mostly alongshore in San Diego) components, respectively, roughly double the values for Santa Barbara (Fig. 9). When a single drifter observa-

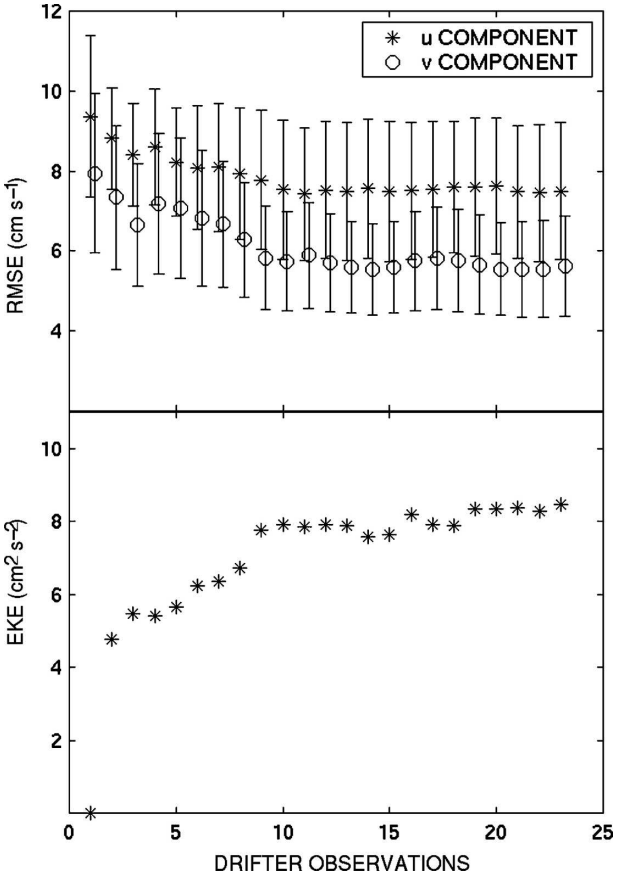


FIG. 9. As in Fig. 8, but for data from San Diego. The HF radar and drifter velocities compared are averages over a 1-km square total box and 1 h. The $u$ (east–west) and $v$ (north–south) velocity components correspond to mainly the across-shore and alongshore directions, respectively; 5 h with at least 23 drifter observations are included in the computations.

tion is randomly selected from each of the hours with at least 23 observations and its velocity is compared with the corresponding HF radar total for the hour, RMS differences increase to 9.3 and 7.9 cm $s^{-1}$, respectively.

Trends in Fig. 9 (as for Santa Barbara), indicate that ~3 cm $s^{-1}$ reduction in RMS velocity difference can be attributed to more representative spatial averaging as the number of drifter observations increases. This difference applies to a total box that is 25% of the total box area considered in Santa Barbara (1 vs 4 $km^2$). RMS difference curves show a flattening after 10 observations suggesting more drifter data will not further decrease the RMS difference. As for Santa Barbara, discrepancies related to GDOP are small since radials are nearly orthogonal in the total box considered.

EKE values in San Diego increase fairly rapidly to roughly 8 $cm^2$ $s^{-2}$ for observations up to 10, and then remain mostly flat, supporting the claim that additional drifter observations have little influence on reduction of RMS difference (Fig. 9). Although both regions show that most of the EKE within a total box is captured with 10 drifter observations during an hour, this is not expected to be a general result. Flow field variance (EKE) is regionally dependent and scales with area.

## 4. Discussion and conclusions

Drifter deployments were designed to measure the high frequency and high wavenumber motions that comprise the time and space averages inherent in HF radar totals. Thus, total grid boxes were seeded with drifters, and a combined drifter and HF radar data analysis was performed on radar totals. Because the total boxes contain radial sectors, it was also possible to evaluate the effects of spatial averaging on the radial estimates. However, the radial analyses use only the drifter data collected in the portions of radial sectors that overlay the total box seeded. Small errors are introduced by this generally slight sampling discrepancy, except for the CI radar, where roughly 40% of the radial sector considered lies outside the limits of the total box seeded. This may account for part of the 9–10 cm $s^{-1}$ RMS differences in the CI radar comparison, the largest observed. A better comparison with radials that optimizes drifter resources would require seeding (and reseeding) drifters in sectors.

A trend of decreasing RMS differences between velocity components measured by HF radar and by drifters occurs as the number of drifter observations used to estimate $u$ and $v$ increases. This trend was found for comparisons conducted with data from both San Diego and Santa Barbara. It indicates that unresolved subgrid-scale velocity variance contributes significantly to differences between velocities observed by HF radars and velocities observed with point measurement approaches such as current meters. Comparisons using single drifter observations give RMS differences near 10 cm $s^{-1}$, consistent with differences reported in previous studies comparing HF radar and current meter measurements (e.g., Janopaul et al. 1982; Schott et al. 1986; Graber et al. 1997; Chapman et al. 1997; Essen et al. 2000; Emery et al. 2004). Here, minimum differences between HF radar and drifter velocities are ~5 cm $s^{-1}$, and occur when 15–30 drifter observations are incorporated into velocity averages. A difference of roughly 3.5 cm $s^{-1}$ is due to sampling domain discrepancies, where comparisons are on different scales.

Part of the RMS velocity differences observed may result from errors in measuring antenna patterns or changes in the patterns through time. The observations presented here indicate the degree to which velocity comparisons can degrade and the time scales over

which the degradation occurs. During July and August 2004, the RMS difference between COP (COP1 and COP2) radials and average drifter velocities is between 3.1 and 4.9 cm $s^{-1}$, among the smallest in this study. Differences are averages for 24 h spread over four different days making coincidental agreement unlikely. In January 2005, the difference increases to 9.1 cm $s^{-1}$, and clearly represents a bias (Fig. 5; Table 3). The reason for degradation in January is most likely the result of a change in antenna patterns, which is known to have occurred between May 2004 and August 2005. Kohut and Glenn (2003) attribute large differences between HF radar and ADCP data to antenna pattern distortions caused by changes in the local environment. Extreme rains in Southern California during the winter of 2004/05 resulted in pronounced changes in vegetation at the COP radar site that may be responsible for the antenna pattern change.

A significant change in radar performance over a few hours was observed in the San Diego data. On 13 April 2005, and the first 2 h sampled on 14 April, the PL radar measures radial velocities that follow the trend of average drifter velocities and, with a single hourly exception, lie well within the scatter of the drifter measurements (Fig. 6). Then, ~20 cm $s^{-1}$ difference occurs during the last two hours (2030 and 2130 UTC). The PL radar also shows a difference of near 20 cm $s^{-1}$ (magnitude) compared with radials collected by the CI radar during this time. The PL and CI radars are expected to give radials of the same magnitude, but in opposite directions. Performance of the PL radar appears to be subject to time-dependent influences that lead to baseline errors in reciprocity between PL and CI. While the short time scale over which RMS differences increase and the fact that it only occurs for the PL radar data seem consistent with effects of radio interference, such noise is not evident in the cross-spectra. Data collected during periods of poor reciprocity are being further investigated.

Radar data in San Diego are processed using both measured and idealized antenna patterns. Examination of RMS differences between drifter and radar data processed using these two methods provides quantification of the improvement with measured patterns in the context of the drifter dataset. Radar measured surface currents processed with idealized beam patterns have RMS differences with drifter averages between 7 and 14 cm $s^{-1}$, with most values greater than 9.5 cm $s^{-1}$ (Table 3). Corresponding biases are between 6 and 11 cm $s^{-1}$ with most values greater than 9.0 cm $s^{-1}$ (Table 3). These values are typically ~5 cm $s^{-1}$ greater, or near double, those determined with radar data processed using measured antenna patterns.

The reduction in RMS velocity differences in the San Diego data with measured antenna patterns supports results of Kohut and Glenn (2003) and Paduan et al. (2007), who attribute errors of more than 10 cm $s^{-1}$ to poorly known antenna patterns. Large changes in radar radials, relative to drifter velocities, may not necessarily be evident in RMS difference. Consider the case where the bias (difference) between platforms goes from positive to negative without changing magnitude. The occasional use of drifter comparisons to determine both bias and RMS difference can indicate errors related to antenna patterns, ultimately improving the quality of HF radar data provided to users.

Applications of HF radar data involve determination of Lagrangian pathways to understand the fate or origin, of pollutants, larvae, and objects lost at sea. This requires knowledge of instantaneous velocities $\mathbf{u}(t, x)$ available from HF radar totals as

$$\mathbf{u}(t, x) = \mathbf{u}_{\text{total}}(\text{t, x}) + \mathbf{u}'(t, x), \tag{3}$$

where $\mathbf{u}_{\text{total}}(\text{t, x})$ is the total HF radar velocity, which is an average over time (t) and space (x), and $\mathbf{u}'(x, t)$ is a largely nondeterministic subgrid-scale velocity component that is not necessarily uniform in space and time [$\mathbf{u}(t, x)$ and $\mathbf{u}'(x, t)$ are defined for an instantaneous time ($t$) and point location ($x$)]. Validation of HF radar data with dense arrays of drifters provides a quantification of both measurement differences and velocity variance that should be incorporated into the first and second terms on the right-hand side of Eq. (3), respectively, for the most accurate determination of pathways from HF radar surface current totals.

*Acknowledgments.* Thanks to Kirk Ireson for managing the fleet of drifters. Dave Farrar, Shane Anderson, Brian Chinn, and Kirk Ireson were always willing to release-and-catch drifters. Comments from two anonymous reviewers helped improve the paper. Reviewer 1 provided especially thoughtful suggestions. This research was supported by the National Science Foundation under Grant OCE-0352187 and the Minerals Management Service, U.S. Department of Interior under MMS Agreement 1435-01-00-CA-31063 to 18212. The views and conclusions contained in this document are those of the authors and should not be interpreted as necessarily representing the official policies, either expressed or implied, of the U.S. government.

## REFERENCES

Barrick, D. E., and B. J. Lipa, 1997: Evolution of bearing determination in HF current mapping radars. *Oceanography,* **10,** 72–75.

——, J. M. Headrick, R. W. Bogle, and D. D. Crombie, 1974: Sea backscatter at HF: Interpretation and utilization of the echo. *Proc. IEEE,* **62,** 673–680.

——, M. W. Evans, and B. L. Weber, 1977: Ocean surface currents mapped by radar. *Science,* **198,** 138–144.

Chapman, R. D., L. K. Shay, H. C. Graber, J. B. Edson, A. Karachintsev, C. L. Trump, and D. B. Ross, 1997: On the accuracy of HF radar surface current measurements: Intercomparison with ship-based sensors. *J. Geophys. Res.,* **102** (C8), 18 737–18 748.

Csanady, G. T., 1982: *Circulation in the Coastal Ocean.* D. Reidel, 279 pp.

Emery, B. M., L. Washburn, and J. A. Harlan, 2004: Evaluating radial current measurements from CODAR high-frequency radars with moored current meters. *J. Atmos. Oceanic Technol.,* **21,** 1259–1271.

Essen, H. H., K. W. Gurgel, and T. Schlick, 2000: On the accuracy of current measurements by means of HF radar. *IEEE J. Oceanic Eng.,* **25,** 472–480.

Frisch, A. S., and B. L. Weber, 1980: A new technique for measuring tidal currents by using a two-site HF Doppler Radar System. *J. Geophys. Res.,* **85,** 485–493.

Graber, H. C., B. K. Haus, R. D. Chapman, and L. K. Shay, 1997: HF radar comparison with moored estimates of current speed and direction: Expected differences and implications. *J. Geophys. Res.,* **102,** 18 749–18 766.

Gurgel, K. W., 1994: Shipborne measurement of surface current fields by HF radar. *L'Onde Electr.,* **74,** 54–59.

——, G. Antonischski, H.-H. Essen, and T. Schlick, 1999: Wellen radar (WERA): A new ground wave radar for remote sensing. *Coastal Eng.,* **37,** 219–234.

Hammond, T. M., C. Pattiaratchi, D. Eccles, M. Osborne, L. Nash, and M. Collins, 1987: Ocean surface current radar vector measurements on the inner continental shelf. *Cont. Shelf Res.,* **7,** 411–431.

Holbrook, J. R., and A. S. Frisch, 1981: A comparison of near-surface CODAR and VACM measurements in the Strait of Juan de Fuca, August 1978. *J. Geophys. Res.,* **86,** 10 908–10 912.

Janopaul, M. M., P. Broche, J. C. de Maistre, H. H. Essen, C. Blanchet, G. Grau, and E. Mittelstaedt, 1982: Comparison of measurements of sea currents by HF radar and by conventional means. *Int. J. Remote Sens.,* **3,** 409–422.

Kaplan, D. M., J. Largier, and L. W. Botsford, 2005: HF radar observations of surface circulation off Bodega Bay (northern California, USA). *J. Geophys. Res.,* **110,** C10020, doi:10.1029/2005JC002959.

Kohut, J. T., and S. M. Glenn, 2003: Improving HF radar surface current measurements with measured antenna beam patterns. *J. Atmos. Oceanic Technol.,* **20,** 1303–1316.

Niiler, P. P., A. L. Sybrandy, K. Bi, P. M. Poulain, and D. Bitterman, 1995: Measurements of the water following capability of holey-sock and TRISTAR drifters. *Deep-Sea Res.,* **42,** 1951–1964.

Ohlmann, J. C., P. F. White, A. L. Sybrandy, and P. P. Niller, 2005: GPS-cellular drifter technology for coastal ocean observing systems. *J. Atmos. Oceanic Technol.,* **22,** 1381–1388.

Paduan, J. D., and L. K. Rosenfeld, 1996: Remotely sensed surface currents in Monterey Bay from shore-based HF radar (Coastal Ocean Dynamics Application Radar). *J. Geophys. Res.,* **101,** 20 669–20 686.

——, K. C. Kim, M. S. Cook, and F. P. Chavez, 2007: Calibration and validation of direction-finding high frequency radar ocean surface current observations. *IEEE J. Oceanic Eng.,* in press.

Roughan, M., E. J. Terrill, J. L. Largier, and M. P. Otero, 2005: Observations of divergence and upwelling around Point Loma, California. *J. Geophys. Res.,* **110,** C04011, doi:10.1029/2004JC002662.

Schmidt, R. O., 1986: Multiple emitter location and signal parameter estimation. *IEEE Trans. Antennas Propag.,* **AP-34,** 276–280.

Schott, F. A., S. A. Frisch, and J. C. Larsen, 1986: Comparison of surface currents measured by HF Doppler Radar in the western Florida straits during November 1983 to January 1984 and Florida current transports. *J. Geophys. Res.,* **91,** 8451–8460.

Shay, L. K., H. C. Graber, D. B. Ross, and R. D. Chapman, 1995: Mesoscale ocean surface current structure detected by high-frequency radar. *J. Atmos. Oceanic Technol.,* **12,** 881–900.

Stewart, R. H., and J. W. Joy, 1974: HF radio measurements of surface currents. *Deep-Sea Res.,* **21,** 1039–1049.

Winant, C. D., E. P. Dever, and M. C. Hendershott, 2003: Characteristic patterns of shelf circulation at the boundary between central and southern California. *J. Geophys. Res.,* **108,** 3021, doi:10.1029/2001JC001302.